Near-infrared downconversion in Eu^{2+} and Pr^{3+} co-doped $KSrPO_4$ phosphor*

Sun Jia-Yue(孙家跃)†, Sun Yi-Ning(孙翊宁), Zhu Ji-Cheng(朱吉成), Zeng Jun-Hui(曾军辉), and Du Hai-Yan(杜海燕)

School of Science, Beijing Technology and Business University, Beijing 100048, *China*

(Received 1 June 2012; revised manuscript received 9 October 2012)

A novel near-infrared (NIR) downconversion (DC) phosphor $KSrPO_4$:Eu^{2+}, Pr^{3+} is synthesized by the conventional high temperature solid-state reaction. The Eu^{2+} acts as an efficient sensitizer for Pr^{3+} in the $KSrPO_4$ host. With broad-band near-ultraviolet light excitation induced by the 4f→5d transition of Eu^{2+}, the characteristic NIR emission of Pr^{3+}, peaking at 974 nm and 1019 nm due to $^3P_0 \rightarrow {}^1G_4$ and $^1G_4 \rightarrow {}^3H_4$ transitions, is generated as a result of the energy transfer from Eu^{2+} to Pr^{3+}. The luminescence spectra in both the visible and the NIR regions and the decay lifetime curves of Eu^{2+} prove the energy transfer from Eu^{2+} to Pr^{3+}. This Eu^{2+} and Pr^{3+} co-doped $KSrPO_4$ phosphor may be a promising candidate to modify the spectral mismatch behavior of crystalline solar cells and sunlight.

Keywords: optical properties, cooperative energy transfer, downconversion

PACS: 78.55.–m, 61.05.cp, 33.50.Dq **DOI:** 10.1088/1674-1056/22/5/057803

1. Introduction

Recently, photovoltaic (PV) generation has attracted much attention because it is a sustainable way to generate electricity.[1] Solar photovoltaic power generation is the core component.[2] Most PV solar cells are made from crystalline silicon, either single-crystal or multi-crystalline silicon. The phosphor material studied in this work can be applied to silicon-based solar cells. The peak of the spectral sensitivity of a c-Si solar cell is at around 1000 nm, corresponding to its band gap 1.1 eV. However, sunlight's emission peak is in the visible region at around 400–700 nm. Most of the energy loss of the solar cells is related to the spectral mismatch: photons with energy smaller than the band gap (E_g) cannot be absorbed (sub-band gap transmission) and a large part of the energy of the photons with energy larger than the band gap is lost as heat (thermalization loss).[3] Therefore, the energy loss attributed to the spectral mismatch can be reduced by adapting the solar spectrum before it is absorbed by the solar cell.

Recently, downconversion (DC) through a cooperative energy transfer (CET) process has attracted growing attention. Moreover, the DC is also known as the quantum cutting (QC) luminescence because one photon can be 'cut' into two photons with smaller energy. In this way, DC materials are capable of harvesting a high-energy visible photon as two near-IR (NIR) photons, so these materials are considered for applications as downconverters to enhance the efficiency of photovoltaic cells.[4] Lanthanide ions are very well suited to use in the DC, since they have a rich energy level structure that allows for an efficient spectral conversion. Downconverters can be divided into ionic-like and band-like downconverters. In band-like downconverters, the absorption takes place via a band-to-band excitation in the host material, and the emission occurs via the energetic levels of the doping ions.[5–7] Meijerink *et al.* pointed out the necessity of a sensitizer that shows strong absorption in the 300–500 nm region and can transfer energy efficiently to the emitter in order to achieve efficient near-infrared quantum cutting.[8] The excitation bands of Tb^{3+}, Tm^{3+}, and Pr^{3+} are very weak and narrow due to the luminescent nature of the 4f→4f transition. Therefore, in order to improve the solar cell efficiency, it is important to explore rare-earth (RE) ion pairs, which show a strong and broad absorption in the ultraviolet/visible (UV/VIS) region and efficiently use the energy to emit more than two photons in the NIR region. Wei *et al.*[9] and Qu *et al.*[10] have reported the broad-band NIR downconversion of Bi^{3+} and Yb^{3+} codoped cubic Y_2O_3.

Eu^{2+} and Ce^{3+} are two promising sensitizer candidates, both of which show broad and strong absorptions in the desired spectral region due to the 4f→5d transition. Broad-band quantum cuttings in Ce^{3+}–Yb^{3+} and Eu^{2+}–Yb^{3+} co-doped systems, in which Ce^{3+} or Eu^{2+} acts as an energy transfer (ET) donor, have been proposed and studied.[11] The Eu^{2+} might be a proper sensitizer ion, as its 4f→5d transition covers a broad spectral range and the energy of the 4f→5d transition can be tuned by changing either the crystal field strength or the covalency of the host.[12–14] Furthermore, since the QC was first presented by Somerdijk *et al.*[15] in 1974, they found that Pr^{3+} in YF_3 can cut one incident vacuum ultravio-

*Project supported by the National Natural Science Foundation of China (Grant No. 20976002), the Beijing Natural Science Foundation, China (Grant No. 2122012), and the Special Funding of the Ministry of Education of Guangdong Province, China (Grant No. 2011B090400100).

†Corresponding author. E-mail: jiayue_sun@126.com

© 2013 Chinese Physical Society and IOP Publishing Ltd

let photon into two visible photons. This downconversion luminescence process has also been found in many Pr^{3+}-doped materials.[16–19]

In the present work, energy transfer and downconversion luminescence are found and investigated in detail for the (Eu^{2+}, Pr^{3+}) couple in $KSrPO_4$ phosphors. The dependencies of the VIS and NIR emissions, decay lifetime, energy transfer efficiency (ETE), and quantum efficiency (QE) on the Pr^{3+} concentration are also discussed.

2. Experiment

All the $KSrPO_4$:Eu^{2+}, Pr^{3+}, K^+ phosphors were prepared by the conventional solid-state reaction. The raw material was a stoichiometric mixture of reagent grade KH_2PO_4 (A.R.), $SrCO_3$ (A.R.), Eu_2O_3 (99.999%), and Pr_2O_3 (99.999%). In general, the different valence states of the rare earth ions and the Pr^{3+} ion require a charge compensation mechanism. For this reason, the host lattice was treated in our experiment with the charge compensator ions K^+. The K_2CO_3 was added as an easy substitute for Sr^{2+} by Pr^{3+}. The composition for each material was prepared in a proper stoichiometric ratio and mixed thoroughly in an agate mortar. First, the mixture was heated up to 600 °C and kept at that temperature for 3 h in air. After that, the samples were thoroughly mixed and heated for 3 h in a CO atmosphere at 1300 °C to insure the complete reduction of Eu^{3+} ions to Eu^{2+}.

The X-ray diffraction (XRD) patterns were obtained on a Shimadzu model XRD-6000 X-ray powder diffractometer with Cu K_α radiation (40 kV, 30 mA). The VIS emission spectrum was recorded using a Hitachi F-7000 fluorescence spectrophotometer, and a 150 W Xe lamp was used as the excitation lamp. The NIR emission and excitation spectrum was recorded using a FluoroLog-3 spectrofluorometer (HORIBA Jobin Yvon, USA) with a 150 W Xe lamp as the excitation lamp and a R1033P photomultiplier for signal detection. Luminescent decay curves were measured by using the FluoroLog-3 spectrofluorometer with Nano LED (N-370) as the excitation source and an R928P photomultiplier for signal detection.

3. Results and discussion

The $KSrPO_4$ host has an orthorhombic crystal structure, and its lattice parameters are $a = 0.7350$ nm, $b = 0.9634$ nm, and $c = 0.5562$ nm. Figure 1 shows the XRD patterns of sample $KSrPO_4$:$0.01Eu^{2+}$, xPr^{3+}, xK^+ ($x = 0.01$, 0.05) and the data of JCPDS card No. 33-1045 for pure orthorhombic $KSrPO_4$ as a reference. No obvious second phase is detected, which indicates that appropriate Eu^{2+}, Pr^{3+} doping and substitution will have little effect on phase formation and structure. This may be attributed to their similar ionic radii (Sr^{2+}, $r = 0.112$ nm; Eu^{2+}, $r = 0.109$ nm; Pr^{3+}, $r = 0.101$ nm).[20] The charge compensation of Pr^{3+} to Sr^{2+} has also been realized by the codoping of K^+. The XRD results indicate that the positions and intensities of XRD peaks agree well with the data for $KSrPO_4$.

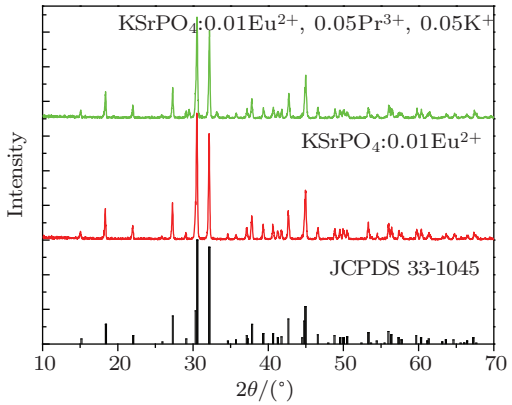


Fig. 1. (color online) XRD patterns of $KSrPO_4$:0.01 Eu^{2+}, $KSrPO_4$:$0.01Eu^{2+}$, $0.05Pr^{3+}$, $0.05K^+$, and the standard data of $KSrPO_4$ (JCPDS No. 33-1045) as a reference.

Figure 2(a) shows the excitation and the emission spectra in the visible region of $KSrPO_4$:$0.01Eu^{2+}$. A broad blue emission band centered at 428 nm is observed under 336 nm excitation. The excitation spectrum consists of a broad band centered at 336 nm due to the $4f^7 \rightarrow 4f^6 5d^1$ transition of Eu^{2+}.[21] The excitation and the emission spectra of Pr^{3+} in $KSrPO_4$ are presented in Fig. 2(b). Three main excitation bands centered at 445 nm, 470 nm, and 482 nm are assigned to the transitions $^3H_4 \rightarrow {}^3P_j$ ($j = 0$, 1, 2) of the Pr^{3+} ions, respectively. Under the 336 nm excitation, three main emission bands centered at 527 nm, 602 nm, and 643 nm can be observed, which are ascribed to the $^3P_0 \rightarrow {}^3H_5$, $^3P_0 \rightarrow {}^3H_6$, and $^3P_0 \rightarrow {}^3F_2$ transitions of the Pr^{3+} ions, respectively.[22,23] The weak band is due to the host absorption. By comparing the excitation emission spectrum of $KSrPO_4$:Pr^{3+} with the emission spectrum of $KSrPO_4$:$0.01Eu^{2+}$, it can be seen that there is a significant spectral overlap in the 440–500 nm region (shown in Figs. 2(a) and 2(b)). Therefore, the effective resonance-type energy transfer from Eu^{2+} to Pr^{3+} is expected. Figure 2(c) gives the excitation and the emission spectra of $KSrPO_4$:$0.01Eu^{2+}$, $0.003Pr^{3+}$ phosphor. The 428 nm emission intensity of Eu^{2+} is very strong, resulting in the 602 nm emission of Pr^{3+} being very weak. The inset shows a magnification of Pr^{3+} luminescence in the 580–700 nm region. The excitation spectra monitored at 428 nm and 602 nm are similar except for the difference in intensity. The presence of the $4f^7 \rightarrow 4f^6 5d^1$ transitions of the Eu^{2+} ions in the excitation spectrum of Pr^{3+} indicates that an efficient ET from Eu^{2+} to Pr^{3+} occurs.

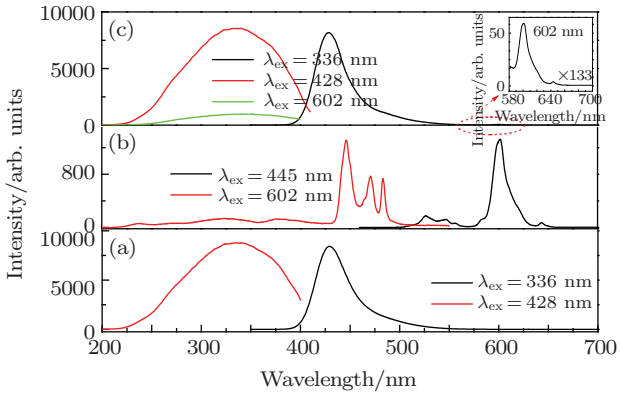


Fig. 2. (color online) Excitation and emission spectra in the visible region of the single-doped and the co-doped samples, (a) $KSrPO_4$:0.01Eu^{2+}, (b) $KSrPO_4$:0.003Pr^{3+}, 0.003K^+, (c) $KSrPO_4$:0.01Eu^{2+}, 0.003Pr^{3+}, 0.003K^+. Inset shows the Pr^{3+} luminescence in the VIS region.

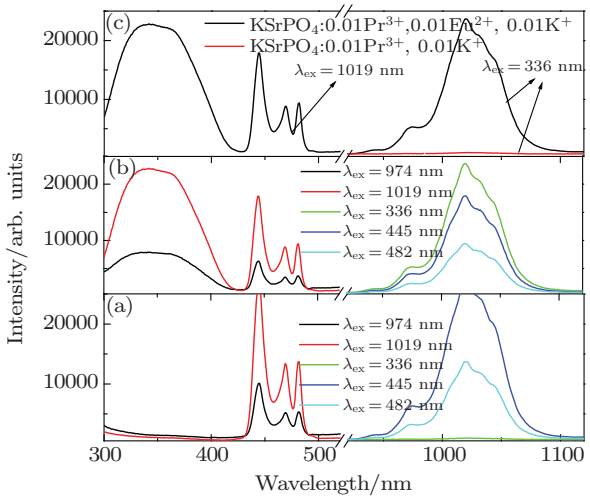


Fig. 3. (color online) Excitation and NIR emission spectra of (a) $KSrPO_4$:0.01Pr^{3+}, 0.01K^+, (b) $KSrPO_4$:0.01Eu^{2+}, 0.01Pr^{3+}, 0.01K^+. (c) For comparison, we also give the excitation (λ_{em} = 1019 nm) and the emission spectra (λ_{ex} = 336 nm) of $KSrPO_4$:0.01Pr^{3+}, $x$$Eu^{2+}$, 0.01$K^+$ ($x = 0, 0.01$).

Figure 3(a) shows the VIS and the NIR emission spectra of $KSrPO_4$:0.01Pr^{3+}, 0.01K^+. It is readily apparent that the Pr^{3+} ions exhibit distinct excitation and NIR-emission features.[24] By examining the NIR emission peak at 1019 nm, we see that the excitation of Pr^{3+} contains several bands centered at 445 nm, 470 nm, and 482 nm (red line), corresponding to the transitions $^3H_4 \rightarrow {}^3P_j$ (j = 0, 1, 2), respectively. A weak band peaking at about 325 nm is probably due to the host absorption. The excitation spectra monitored at 974 nm and 1019 nm are similar except for the difference in intensity. When excited at 336 nm, 445 nm, 482 nm respectively, there is a characteristic NIR emission peaking at 1019 nm, which is assigned to the $^1G_4 \rightarrow {}^3H_4$ electronic transition of Pr^{3+}, and the emission around 974 nm is a second-order peak that can be assigned to the $^3P_0 \rightarrow {}^1G_4$ electronic transition of Pr^{3+},[25] as shown in Fig. 3(b). For comparison, we also give the excitation and the emission spectra of $KSrPO_4$:0.01Pr^{3+}, x0.01Eu^{2+}, 0.01K^+ ($x = 0, 0.01$). From Fig. 3(c) we find that the Pr^{3+} NIR emission intensity of the $KSrPO_4$:0.01Pr^{3+}, $x$$Eu^{2+}$, 0.01$K^+$ system under 336 nm excitation is about 20 times as strong as that of $KSrPO_4$:0.01Pr^{3+}, 0.01K^+, which confirms the highly efficient excitation and subsequent cooperative ET in the presently investigated material.

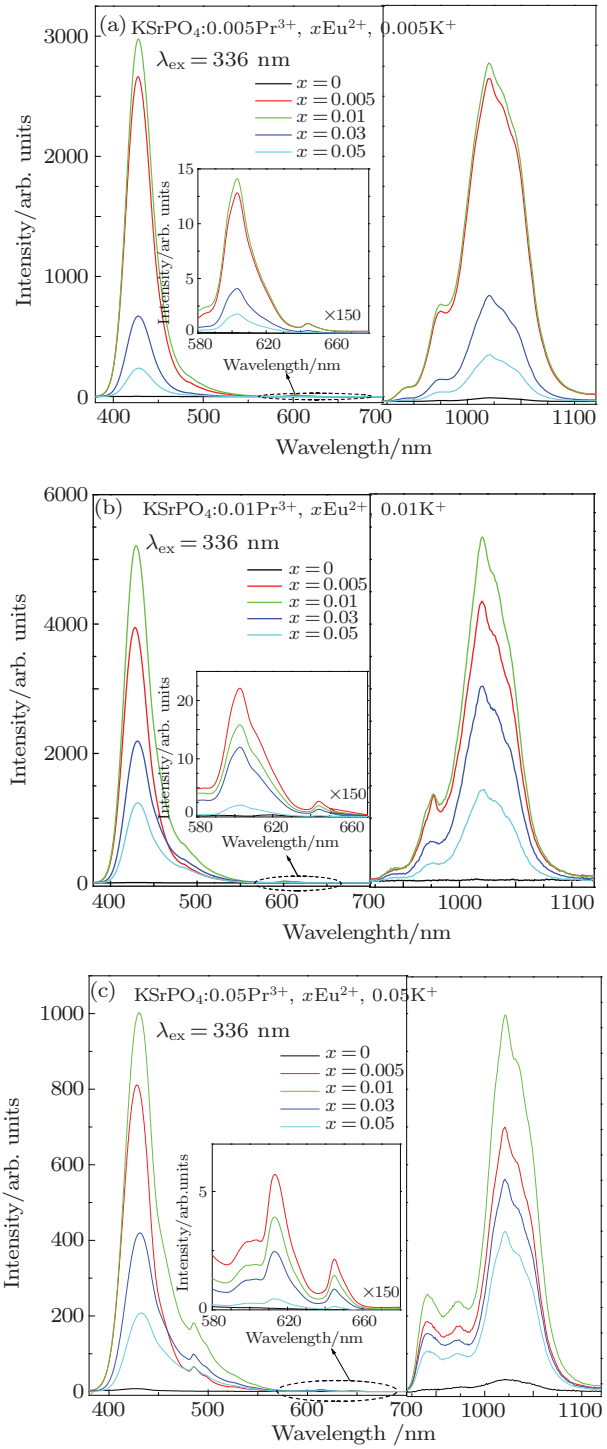


Fig. 4. (color online) Emission spectra of (a) $KSrPO_4$:0.005Pr^{3+}, $x$$Eu^{2+}$, 0.005$K^+$, (b) $KSrPO_4$:0.01Pr^{3+}, $x$$Eu^{2+}$, 0.01$K^+$, and (c) $KSrPO_4$:0.05Pr^{3+}, $x$$Eu^{2+}$, 0.05$K^+$ ($0 \le x \le 0.05$) in the VIS region from 380 nm to 700 nm and the NIR region from 900 nm to 1100 nm (λ_{ex} = 336 nm). The inset shows the Pr^{3+} luminescence in the VIS region.

Figure 4 shows the emission spectra of (a) $KSrPO_4$:0.005Pr^{3+}, $x$$Eu^{2+}$, 0.005$K^+$, (b) $KSrPO_4$:0.01Pr^{3+}, $x$$Eu^{2+}$, 0.01$K^+$, and (c) $KSrPO_4$:0.05Pr^{3+}, $x$$Eu^{2+}$, 0.05$K^+$ ($0 \le x \le 0.05$). Under the 336 nm excitation, the intense characteristic emission peaks of Eu^{2+} and Pr^{3+} are observed in the emission spectra of all samples. As the Eu^{2+} concentration increases, the emission intensities of both Eu^{2+} and Pr^{3+} increase systematically, and reach maxima when x is about 0.01, then decline dramatically. Furthermore, the emission intensity of the Pr^{3+} and Eu^{2+} co-doped $KSrPO_4$ phosphor is higher than that of single doped Pr^{3+}. A similar phenomenon can be found in Figs. 4(b) and 4(c). Therefore the optimum concentration of Eu^{2+} in the Pr^{3+} and Eu^{2+} co-doped material is 1 mol%. The emission spectra of phosphors doped with different concentrations of Pr^{3+} at the fixed 0.01 mol Eu^{2+} concentration are shown in Fig. 5.

The emission spectra of $KSrPO_4$:0.01Eu^{2+}, $x$$Pr^{3+}$, $x$$K^+$ in the VIS and the NIR regions excited at 336 nm are presented in Fig. 5. Compared to the emission spectra in the VIS region of Eu^{2+} and the NIR region of Pr^{3+}, we find that the VIS emission intensity of Eu^{2+} decreases monotonously with the increasing concentration of Pr^{3+}. Meanwhile, it is found that the NIR luminescence intensity of Pr^{3+} increases at first, reaching its maximum at $x = 1$ mol%. Then with the increase of the Pr^{3+}concentration, the emission intensity decreases, which can be attributed to the concentration quenching effect of Pr^{3+}.[25] Therefore, an effective energy transfer from Eu^{2+} to Pr^{3+} is to be expected. The inset of Fig. 5 shows the Pr^{3+} luminescence in the VIS region from 580 nm to 700 nm. Two visible emission bands centered at 602 nm and 643 nm can be observed, which are ascribed to the $^3P_0 \rightarrow {}^3H_6$ and $^3P_0 \rightarrow {}^3F_2$ transitions of the Pr^{3+} ions, respectively. This phenomenon further supports the existence of the ET from Eu^{2+} to Pr^{3+}.[26]

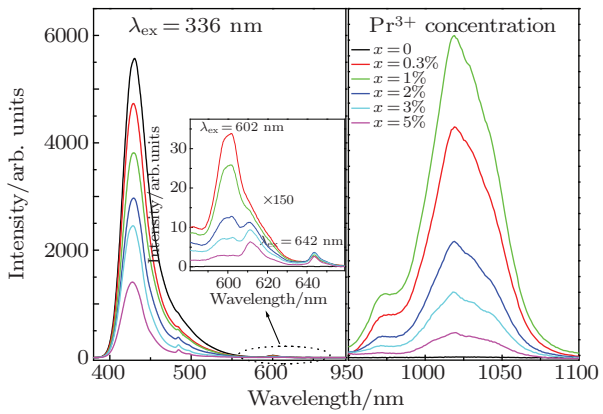


Fig. 5. (color online) Emission spectra of $KSrPO_4$:0.01Eu^{2+}, $x$$Pr^{3+}$, $x$$K^+$ ($0 \le x \le 0.05$) in the VIS region from 380 nm to 700 nm and the NIR region from 900 nm to 1100 nm ($\lambda_{ex} = 336$ nm). The inset shows the Pr^{3+} luminescence in the VIS region.

To further prove the existence of the energy transfer from Eu^{2+} to Pr^{3+}, we depict in Fig. 6 the luminescence decay curves of Eu^{2+} ascribed to the $4f^65d^1 \rightarrow 4f^7$ emission at 428 nm for $KSrPO_4$:Eu^{2+}, Pr^{3+}, K^+ doped with different Pr^{3+} concentrations under the 370 nm excitation. For the sample without Pr^{3+}, a nearly single-exponential luminescence decay is found with a lifetime of 0.552 μs. Obviously, the decay time decreases rapidly with the increase of Pr^{3+} concentration from 0 to 5 mol%, and the decay curve becomes nonexponential for Eu^{2+}–Pr^{3+} co-doped samples. The nonexponential character is attributed to the variation in the distribution of Pr^{3+} acceptor ions around Eu^{2+}. Thus it results in a variety of ET rates for different Eu^{2+}. It is found that the luminescence decay curves of Eu^{2+} show the nonexponential characteristics (Fig. 6), and the energy transfer efficiency η_{ETE} and the total theoretical QE η_{QE} (regardless of energy loss)[27] can be calculated by the following equations:[28,29]

$$\eta_{ETE} = \eta_{x\%\,Pr} = 1 - \frac{\int I_{x\%\,Pr}\,dt}{\int I_{0\%\,Pr}\,dt}, \quad (1)$$

$$\eta_{QE} = \eta_{Eu}(1 - \eta_{x\%\,Pr}) + 2\eta_{x\%\,Pr}, \quad (2)$$

where I denotes the emission intensity of Pr^{3+}, x% Pr stands for the Pr^{3+} concentration, and η_{Eu} stands for the luminescence QE of Eu^{2+} and is set to 1. The lifetimes of the samples are determined to be 0.552 μs, 0.503 μs, 0.464 μs, 0.398 μs, 0.344 μs, and 0.298 μs for samples with 0 mol%, 0.3 mol%, 1 mol%, 2 mol%, 3 mol%, and 5 mol% Pr^{3+}, respectively. The decay lifetimes and the ETE each are plotted as a function of the Pr^{3+} doping concentration in the inset of Fig. 6. We can see that the ETE increases monotonously and reaches a maximum value of 59% when the doping concentration of Pr^{3+} is 5 mol%. The reduced sample lifetime can be ascribed to the energy transfer from Eu^{2+} to Pr^{3+}. Therefore, the ET from Eu^{2+} to Pr^{3+} in $KSrPO_4$:0.01Eu^{2+}, $x$$Pr^{3+}$, $x$$K^+$ ($0 \le x \le 0.05$) is proved.

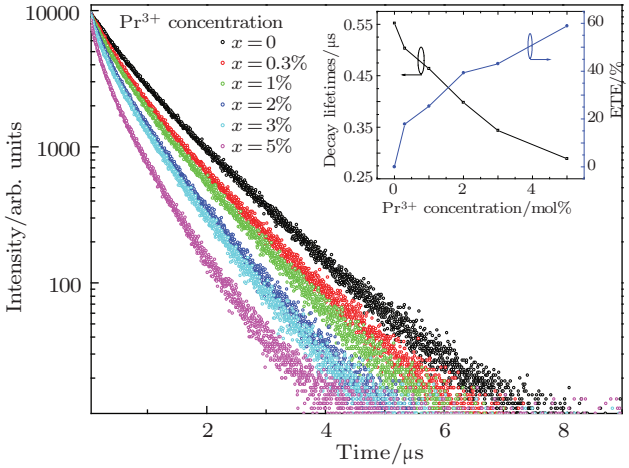


Fig. 6. (color online) Decay curves of the Eu^{2+}:$4f^65d^1 \rightarrow 4f^7$ luminescence ($\lambda_{em} = 428$ nm) under the 370 nm excitation. The different fractions x of Pr^{3+} in the samples are indicated. Inset shows decay lifetime and ETE as a function of the Pr^{3+} doping concentration.

For $KSrPO_4$:0.01Eu^{2+}, 0.01Pr^{3+}, 0.01K^+ phosphors, the QE has been found to be about 159%. The low ETE of

$KSrPO_4$:0.01Eu^{2+}, xPr^{3+}, xK^+ ($0 \leq x \leq 0.05$) phosphors may be ascribed to the inefficient excitation of Pr^{3+} for the phosphors' forbidden transition or the low absorption cross-sections for UV–VIS photons.[29]

The schematic energy levels with the transitions that may be involved in the ET process from Eu^{2+} ions to Pr^{3+} ions in $KSrPO_4$ phosphors are given in Fig. 7. The Eu^{2+} ions absorb energy from the excitation source and are excited to the $4f^65d^1$ level. We give the most likely energy transfer path based on our experiments. Then, the Eu^{2+} ions are relaxed to the split excited state along with a Stokes shift. The emission occurs through the parity-allowed transition from the excited state to the ground state $4f^7$.[30] After the excitation of the Eu^{2+} $4f^65d^1$ states, the electrons can either relax radiatively to the 4f ground state, producing a broadband luminescence in the visible range, or resonance transfer to Pr^{3+} by activating Pr^{3+} from the ground $^3H_4$ level to the excited $^3P_2$ (445 nm), $^3P_1/^1I_6$ (470 nm), or $^3P_0$ (482 nm) level. Then they relax to the emitting level $^3P_0$, in which the process of NIR QC ($^3P_0 \rightarrow {}^1G_4 \rightarrow {}^3H_4$) occurs. Thus two NIR photons are emitted whenever one visible photon is absorbed.

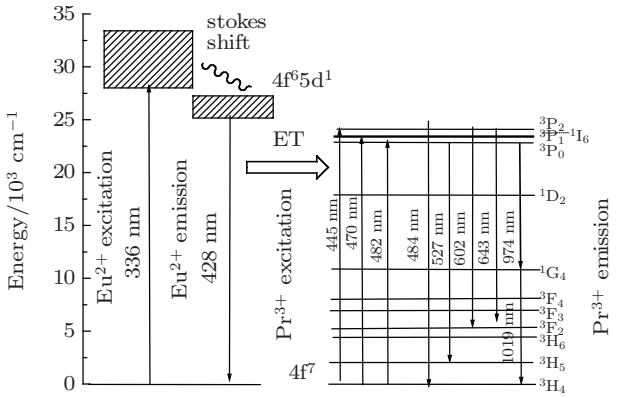


Fig. 7. Schematic energy-level diagram of ET process from Eu^{2+} to Pr^{3+} in $KSrPO_4$:0.01Eu^{2+}, xPr^{3+}, xK^+ phosphors.

4. Conclusion

In summary, Eu^{2+} and Pr^{3+} co-doped $KSrPO_4$ phosphors were successfully synthesized by the conventional high temperature solid-state technique. An XRD analysis was carried out to prove the phase purity. The emission spectra prove the existence of an energy transfer from Eu^{2+} to Pr^{3+} that leads to 900–1100 nm infrared emission and the visible luminescence of Eu^{2+} from 350 nm to 500 nm. The Eu^{2+} ions correspond to a broad blue emission band centered at 428 nm, and Pr^{3+} is at 1019 nm with a second-order peak at 974 nm. The lifetime of Eu^{2+} drops rapidly with the increasing Pr^{3+} concentration, and the energy efficiency increases until 5 mol% Pr^{3+} is introduced, where it reaches the maximum of 59%. As for the energy of the NIR emission just above the band gap of crystalline Si, the spectral conversion material studied in this work may have practical applications in high efficiency silicon-based solar cells.

References

[1] Shockley W and Queisser H J 1961 *J. Appl. Phys.* **32** 510
[2] Xiao W B, He X D, Zhang Z M, Gao Y Q and Liu J T 2012 *Chin. Phys. B* **21** 067304
[3] Strumpel C, McCann M, Beaucarne G, Arkhipov V, Slaouic A, Svrcek V, Canizo C del and Tobias I 2007 *Sol. Energy Mater. Sol. Cells* **91** 238
[4] Trupke T, Green M A and Wurfel P 2002 *J. Appl. Phys.* **92** 1668
[5] Kringlebotn J T, Morkel P R, Reekie L, Archambault J L and Payne D N 1993 *IEEE Photonics Technol. Lett.* **5** 1162
[6] Wegh R T, Donker H, Oskam K D and Meijerink A 1999 *Science* **283** 663
[7] Kasuya R, Isobe T, Kuma H and Katano J 2005 *J. Phys. Chem. B* **109** 22126
[8] Van der Ende B M, Aarts L and Meijerink A 2009 *Phys. Chem.* **11** 11081
[9] Wei X T, Zhao J B, Chen Y H, Yin M and Li Y 2010 *Chin. Phys. B* **19** 077804
[10] Qu M H, Wang R Z, Chen Y, Zhang Y, Li K Y and Yan H 2012 *J. Lumin.* **132** 1285
[11] Zhou J J, Zhuang Y X, Ye S, Teng Y, Lin G, Zhu B, Xie J H and Qiu J R 2009 *Appl. Phys. Lett.* **95** 141101
[12] Liu X F, Teng Y, Zhuang Y X, Xie J H, Qiao Y B, Dong G P, Chen D P and Qiu J R 2009 *Opt. Lett.* **34** 3565
[13] Chen D Q, Wang Y S, Yu Y L, Huang P and Weng F Y 2008 *J. Appl. Phys.* **104** 116103
[14] Ueda J and Tanabe S 2009 *J. Appl. Phys.* **106** 043101
[15] Sommerdijk J, Bril A and de Jager A W 1974 *J. Lumin.* **8** 341
[16] Trupke T, Green M A and Wurfel P 2002 *J. Appl. Phys.* **92** 1668
[17] Richards B S 2006 *Sol. Energy Mater. Sol. Cells* **90** 1189
[18] Strek W, Deren P and Bednarkiewicz A 2000 *J. Lumin.* **87** 999
[19] Zhang Q Y, Yang G F and Jiang Z H 2007 *Appl. Phys. Lett.* **91** 051903
[20] Wu Z C, Shi J X, Wang J, Gong M L and Su Q 2006 *J. Solid State Chem.* **179** 2356
[21] Tang W J and Chen D H 2009 *J. Am. Ceram. Soc.* **92** 1059
[22] Liu T C, Cheng B M, Hu S F and Liu R S 2011 *Chem. Mater.* **23** 3698
[23] De Mello Donega C, Ellens A, Meijerink A and Blasse G 1993 *J. Phys. Chem. Solids* **54** 293
[24] Chen Q J, Zhang W J, Huang X Y, Dong G P, Peng M Y and Zhan Q Y 2012 *J. Alloys Compd.* **513** 139
[25] Zhang G G, Liu C M, Wang J, Kuang X J and Su Q 2012 *J. Mater. Chem.* **22** 2226
[26] Xia Z G, Luo Y, Guan M and Liao L B 2012 *Opt. Express* **20** 722
[27] Chen X B, Kang D G, Li S, Wen L, Yu C L, Hu L L and Zhou J 2011 *Chin. Phys. B* **20** 027801
[28] Engholm M, Norin L and Aberg D 2007 *Opt. Lett.* **32** 3352
[29] Vergeer P, Vlugt T J H, Kox M H F, Den Hertog M I, van der Eerden J P J M and Meijerink A 2005 *Phys. Rev. B* **71** 014119
[30] Zhou J J, Teng Y, Lin G, Xu X Q, Ma Z J and Qiu J R 2010 *J. Electrochem. Soc.* **157** B1146